Development of Macrostructural Effects of Cold Drawing on Nylon 6 Fibers

I. M. Fouda, F. M. El-Sharkawy

Physics Department, Faculty of Science, Mansoura University, Mansoura, Egypt

Received 22 August 2003; accepted 26 April 2004
DOI 10.1002/app.20897
Published online in Wiley InterScience (www.interscience.wiley.com).

ABSTRACT: This work reports measurement of the molecular orientation by two techniques for nylon 6 fibers drawn at room temperature. The changes in the strain and optical parameters are used to obtain some macrostructural parameters to evaluate the cold-drawing process values of the mechanical orientation functions, $[P_2(\cos\theta)]$, $[P_4(\cos\theta)]$, amorphous and crystalline orientation functions (F_c and F_a), and the molar number of chain segments per unit volume (N_e). Also the crosslink density (N_0), the chain entanglement density (N_s), the average optical orientation F_{av}, the dielectric constant (ε), the dielectric susceptibility (η), the shrinkage stress (k_s), and other parameters were calculated. Relationships between the calculated parameters are given. The present study demonstrates changes in the molecular reorientation factors and the obtained new physical properties resulting from cold-drawing process. © 2004 Wiley Periodicals, Inc. J Appl Polym Sci 94: 287–295, 2004

Key words: nylon; crystallinity; orientation; crosslinking; dielectric properties

INTRODUCTION

Cold drawing occurs in both crystalline and amorphous polymers. Cold drawing occurs at temperatures below the glass transition, sometimes as much as almost 150°C below. It has been suggested by Andrews and others[1–3] that the yield process and subsequent cold drawing do not involve long-range molecular flow but are associated with molecular rearrangements between points of entanglement and/or crosslinkage. It is known that strain hardening is a necessary prerequisite for cold drawing and there are two possible sources of strain hardening in polymers:

1. Strain-induced crystallization may occur at the high degree of extension occurring in cold drawing. The occurrence of crystallization on cold drawing is probably dependent on raising the local temperature in the specimen sufficiently to permit the necessary molecular mobility for the required structural reorganization.
2. There is a change in the directional properties as the molecular orientation changes during drawing, such that the stiffness increases along the drawing direction, a general phenomenon that is true for both crystalline and amorphous polymers. It is also clear that, although the general effect of drawing is to produce some degree of molecular alignment parallel to the draw direction, the morphological changes are complex.

As in the measurement of degree of crystallinity, the determination of degree of orientation is complicated both by the complexity of the types of orientation that can occur and by the conceptual difficulties involved in the current picture of the structure of an oriented specimen. The interpretation of the measurements depends on the model and simplifying assumptions in each method, but these differences are relatively minor, and the agreement among results by different methods is generally satisfactory. Birefringence is one of the most sensitive indicators of the extent of the anisotropy of properties of polymers and therefore the degree of macromolecular orientation.

Birefringence (i.e., change in index of refraction with directions) is evidenced by the ability of a material to rotate the plane of polarized light. The birefringence of a crystalline polymer is composed of contributions from the crystalline and amorphous regions plus a contribution, from birefringence, resulting from the shape of the crystals or the presence of voids. For completely unoriented material, the contributions of the crystalline and the amorphous regions are both zero.[4–7]

The technical and commercial importance of nylon 6 has long been recognized. Many of its physical properties have been extensively investigated. The improvement of the mechanical properties of nylon fibers is an important assignment. Many techniques leading to high-modulus and high-strength fibers

Correspondence to: I. Fouda (ifouda@yahoo.com).

have so far been proposed and discussed extensively elsewhere.[8–10]

When drawing synthetic fibers, the decrease of the cross section is not uniform along the length of a fiber. At certain places, the fiber becomes thin and elongated, which is known as necking, and the neck moves along the fiber on further stretching. The relationships of neck geometry and neck propagation to the stress, strain, and stress rate have been studied extensively.[11–16] Deformation is accompanied by a strong exothermal effect, in which the local temperature increases 20–30°C, which makes local deformation easier. The structural changes thus formed affect various properties of the fibers finally obtained. The purpose of this study was to apply the cold-drawing process to nylon 6 fibers to improve the mechanical properties and to discuss the effect of microstructure on the optical parameters.

Theoretical considerations

The use of a Pluta interference microscope, with totally duplicated image of the fiber to measure the mean refractive indices nylon 6 in the parallel and perpendicular directions, was discussed in detail elsewhere.[17–21]

Following Hermans[5] and Ward,[7] we can evaluate the shrinkage, stress, the mechanical orientation factors $[P_2(\cos\theta)]$ and $[P_4(\cos\theta)]$, and the average optical orientation factor; and, following the optical parameter equations used previously,[16–19] the dielectric constant (ε), the dielectric susceptibility (η), and the surface reflectivity (R') as well.

EXPERIMENTAL

Material

The original material used in this study was as-spun nylon 6 fibers supplied by Kafr El-Dawar, Egypt. The original fiber had a diameter of 0.0205, mm, a degree of crystallinity of 45.91%, and a birefringence of 0.0077. The original fiber was found to be anisotropic from optical measurements.

Application of two-beam interferometry

A microstrain device was described before and used in conjunction with a two-beam polarizing interference Pluta microscope. It was modified to measure both stress and strain[17–20] and was used to measure both the refractive indices for the two principal vibration directions and the birefringence values as a function of stress–strain, and draw ratio of nylon 6 fibers. The Pluta microscope gives either a uniform field or a fringe interference field with continuously variable amount and direction of lateral image duplication. The microscope can also be adjusted to give a nonduplicated image representing a subtracted image from which the birefringence can be determined. The fiber was fixed at its ends and stretched during the measurement process at room temperature 29°C with the designed and constructed manipulation device described previously.[21]

Isotropic refractive index[22]

Because most macromolecular crystals are birefringent, an appropriate average refractive index must be used and can be given by the following equation:

$$n_{\text{iso}} = (n_{\perp}^2 n_{\parallel})^{\frac{1}{3}} \tag{1}$$

Density

The density (ρ) of the drawn fiber was calculated by using the Gaur–de Vries formula[23]:

$$\rho = \frac{1}{0.275}\left(\frac{\bar{n}^2-1)}{(\bar{n}^2+2)}\right. \tag{2}$$

where $\bar{n}$ is the mean refractive index. We used eq. (2) in our present work for evaluating the crystallinity of cold-drawn nylon 6 fibers because it is the only the available technique at the present time.

Degree of crystallinity

The crystallinity in weight fraction (X_v) was obtained with the following relation:

$$X_v = \frac{\{\rho_c(\rho - \rho_a)\}}{\{\rho(\rho_c - \rho_a)\}} \times 100 \tag{3}$$

where ρ_c and ρ_a are the densities of the crystallinity and amorphous phases, respectively. In this estimation, values of 1.230 and 1.084 g/cm^3 were assumed for ρ_c[24] and ρ_a, respectively.[25]

Amorphous orientation

The amorphous orientation function F_a was calculated by combining the two models of Samuel and Gaylord for the crystalline orientation F_c. The Gaylord model is in good agreement with experimental data on nylon 6, as follows[26]:

$$F_a = \frac{\Delta n - \Delta n_c^{\circ} F_c X_v}{\Delta n_a^{\circ}(1 - X_v)} \tag{4a}$$

The crystalline orientation factors F_c were evaluated by using the following equation:

$$F_c = \frac{(D^3 - 1)}{(D^3 + 2)} \tag{4b}$$

where D is the draw ratio; Δn is the total birefringence of the fiber; X_v is the volume fraction crystallinity; and Δn_c° and Δn_a° are the intrinsic birefringence of the crystalline and noncrystalline regions, respectively. The values of Δn_c° and Δn_a° were 0.0780 and 0.0689,[27] respectively.

Average optical orientation[28]

The overall orientation F_{av} was calculated from birefringence measurements on individual fibers. Optical birefringence gives the average of crystalline and amorphous orientation. Orientation frequently means orientation of ordered phases. It has to be stressed, however, that both crystalline and amorphous materials can exist in both oriented and unoriented states. The average orientation F_{av} was calculated from the following equation:

$$F_{av} = \left(\frac{2\Delta n}{\Delta n_c^\circ + \Delta n_a^\circ}\right) \tag{5}$$

where the denominator is composed of the intrinsic birefringence of both the crystalline and the amorphous regions.

The stress optical coefficient[29]

The value of the stress-optical coefficient C_s is dependent on the chemical structure of the polymer. Also, the value of this coefficient depends solely on the mean refractive index and the optical anisotropy of the random link, as seen from the following equation[26]:

$$C_s = \frac{2\pi}{45KT}\frac{(\bar{n}^2 + 2)^2}{\bar{n}}(\alpha_1 - \alpha_2) \tag{6}$$

where α_1 and α_2 are the polarizabilities along and across the axes of such units.

$$C_s = \frac{\Delta n}{\sigma} \tag{7}$$

Also C_s is independent of the chain length and the degree of crosslinking. From the above equation it can be seen that birefringence in elastomers is proportional to the applied stress.

Number and functionality of crosslinks[30]

For uniaxial tensile stress, the following equation relates the stress to the elongation:

$$\sigma = N_e RT(D^2 - D^{-1}) \tag{8}$$

where σ is the stress; R is the gas constant; T is the absolute temperature; and N_e is the molar number of chain segments per unit volume and equals $\rho/\bar{M}_c$, where $\bar{M}_c$ is the number-average molar mass of the chains between the crosslinks and ρ is the density. The modulus N_eRT increases in a linear manner with increasing temperature. The other important aspect of eq. (8) is that the modulus is inversely proportional to $\bar{M}_c$. The modulus $\rho RT/\bar{M}_c$ is proportional to the absolute temperature and increases with increasing crosslink density (i.e., with increasing $\bar{M}_c$). Also it is of particular interest to show that the elastic constant G is equivalent to shear modulus; thus, this constant may be expressed as follows:

$$G = \frac{\rho RT}{\bar{M}_c} = NKT$$

where N is the number of chain per unit volume and K is Boltzmann's constant. The shear elastic modulus is related to Young's modulus for elastic materials when Poisson's ratio is about 0.5, so that the elastic tensile modulus is three times greater than shear modulus.

Mooney–Rivlin constants[32]

To fit the Ball model[29] to the experimental data, initial estimates of the model parameters are needed. These were obtained using Mooney–Rivlin plots, where the reduced stress

$$\sigma^* = \frac{\sigma}{[D_{\max}^2 - D_{\min}^2]} \tag{9}$$

is plotted against the inverse of the draw ratio, which gives a linear plot for rubberlike behavior. Therefore

$$\sigma^* = (C_1 + C_2 D^{-1}) \tag{10}$$

where C_1 and C_2 are empirical constants, called Mooney–Rivlin coefficients, which can be related approximately to the structure of the network parameters, N_0, the crosslink density, and N_s, the chain entanglement density, where

$$N_0 = C_1/KT \tag{11a}$$

and

$$N_s = C_2/KT \tag{11b}$$

where K is Boltzmann's constant. The estimate of N_s, however, is not strictly correct because C_2 also relates

to the link effectiveness. Even as the Mooney–Rivlin plots obtained from the deformation of nylon 6 fiber are not linear over the whole strain range, so the data points on the initial linear part of the curve were used to give values of $N_0 = 5.988 \times 10^{17}$ and $N_s = 1.205 \times 10^{15}$.

Shrinkage stress

The shrinkage on fibers is related to the extension ratio D (final fiber length/starting length) by the following relation[7]:

$$k_s = (D - 1)D \tag{12}$$

This gives $D = 1/(1 - k_s)$, which explains the use of the factor $\{1/(1 - k_s)^2 - (1 - k_s)\}$ as the ordinate in this figure. If the shrinkage force could be measured, the stress optical coefficient can be used to calculate the number of monomer units per link.

Calculation of dielectric constant and dielectric susceptibility

The dielectric constant ($\varepsilon_\perp$), measured radially, is different from that ($\varepsilon_\parallel$) measured axially. The fiber has two different dielectric constants and is anisotropic with respect to its dielectric[33]

$$\varepsilon = \frac{1 + 2(\bar{n}^2 - 1/\bar{n}^2 + 2)}{1 - (\bar{n}^2 - 1/\bar{n}^2 + 2)} \tag{13}$$

and analogous equations for $\varepsilon_\parallel$ and $\varepsilon_\perp$. The dielectric constant of fibers varies according to the way in which fibers are arranged (i.e., to the degree of orientation).

The dielectric susceptibility η is related to ε by the well-known equation[17]

$$\eta = \frac{\varepsilon - 1}{4\pi} \tag{14}$$

and analogous equations for $\eta_\parallel$ and $\eta_\perp$.

Surface reflectivity[34]

The surface reflectivity of polymer for light at normal incidence can be estimated from Fresnel's equation and knowledge of the mean refractive index $\bar{n}$. Thus the percentage reflection R' is given by

$$R' = \left(\frac{\bar{n} - 1}{\bar{n} + 2}\right)^2 \times 100 \tag{15}$$

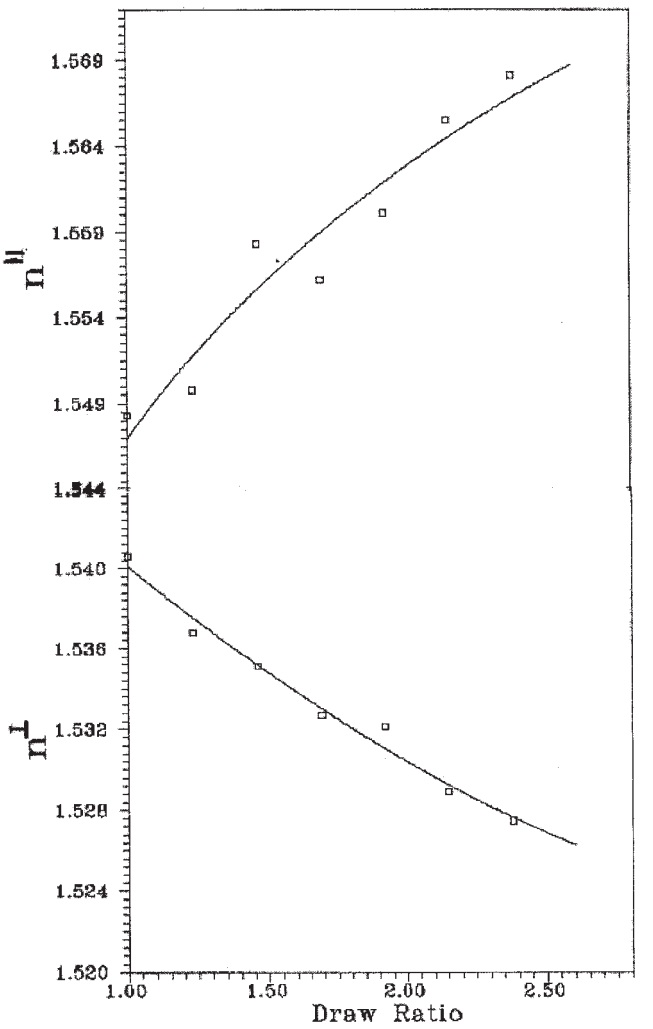

Figure 1 Relationship between the mean refractive indices ($n_a^\parallel$ and $n_a^\perp$) and draw ratio for nylon 6 fiber.

RESULTS AND DISCUSSION

The totally duplicated image of the fibers obtained with a Pluta polarizing interference microscope was used to calculate the mean refractive indices $n_a^\parallel$ and $n_a^\perp$ of nylon 6 fibers. Plane polarized light of $\lambda = 546$ nm and a liquid of refractive index $n_L = 1.5445$ at 20°C were used. The corresponding draw ratios are 1.23, 1.69, and 2.15, respectively. At different draw ratios the mean refractive indices and birefringence were calculated. Figure 1 shows the relationship between the mean refractive indices ($n_a^\parallel$ and $n_a^\perp$) and draw ratio for nylon 6 fibers, where $n_a^\parallel$ values increase as the draw ratio increases and $n_a^\perp$ values decrease with increasing draw ratio.

Figure 2 shows the relationship between the Δn_a and draw ratio for nylon 6 fibers, where Δn_a increases as D increased and optical and structural parameters, such as isotropic refractive index (n_{iso}), were calculated. The resultant data of this parameter are given in Table I at different draw ratios for nylon 6 fibers.

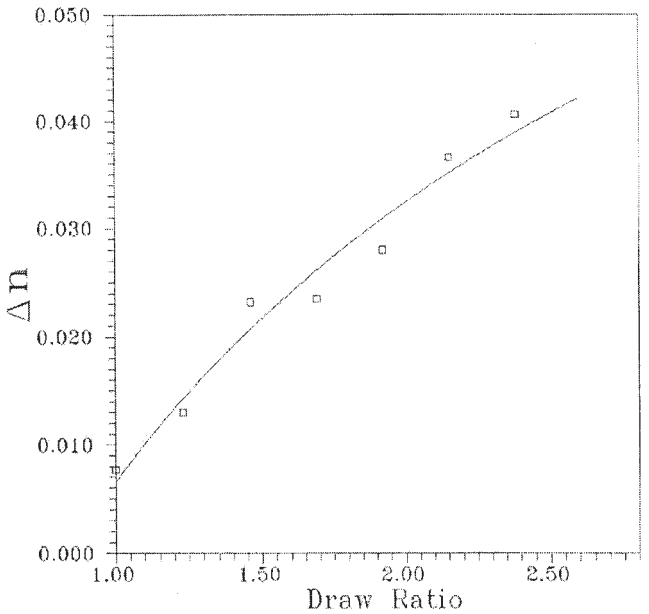

Figure 2 Relationship between the birefringence Δn and draw ratio for nylon 6 fiber.

Figure 3 shows the relationship between the orientation functions [$P_2(\theta)$ and $P_4(\theta)$] and draw ratio for nylon 6 fibers, showing a decrease in the two functions as the draw ratio increased.

The dielectric constant ε and the dielectric susceptibility η were determined from eqs. (11) and (12). The resultant data for $\varepsilon^{\parallel}$, $\varepsilon^{\perp}$, $\bar{\varepsilon}$, $\eta^{\parallel}$, $\eta^{\perp}$, and $\bar{\eta}$ are given in Table I, where $\varepsilon^{\parallel}$ and $\eta^{\parallel}$ are increased because of an increase of draw ratios and $\varepsilon^{\perp}$ and $\eta^{\perp}$ are decreased, whereas $\bar{\varepsilon}$ and $\bar{\eta}$ changed because of an increase of draw ratios.

Figure 4 shows the changes between crystallinity X_v and draw ratio for nylon 6 fibers. X_v increased and decreased because of changes in the fluctuation of thermodynamic changes associated with changes in stress.

Figures 5, 6, and 7 show the relationship between the amorphous orientation functions F_a, the crystalline orientation function F_c, and draw ratio for nylon 6 fibers. F_a and F_c increased as the draw ratio increased

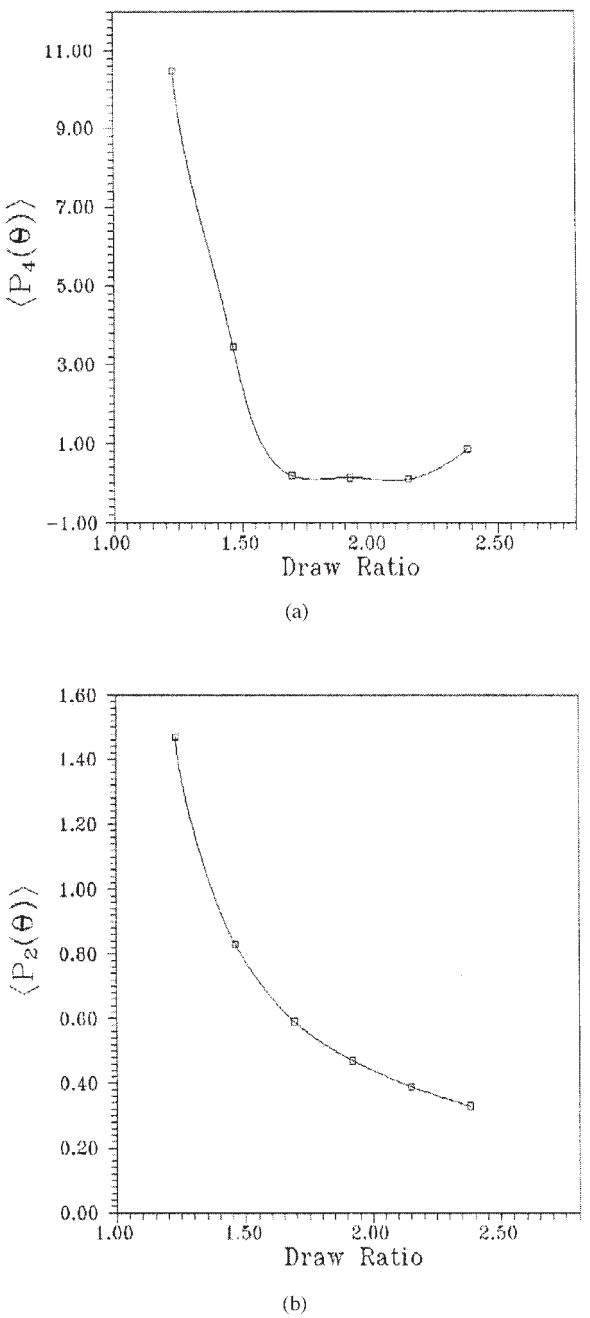

Figure 3 Relationship between the orientation functions $\langle P_2(\cos\theta)\rangle$ and $\langle P_4(\cos\theta)\rangle$ and drawratio for nylon 6 fiber.

TABLE I
Values of Draw Ratios, Isotropic Refractive Index (n_{iso}), Tensile Stress (σ), Dielectric Constant ($\varepsilon^{\parallel}$, $\varepsilon^{\perp}$, and $\bar{\varepsilon}$), Dielectric Susceptibility ($\eta^{\parallel}$, $\eta^{\perp}$, and $\bar{\eta}$), Along and Across the Fiber Axis, and Surface Reflectivity (R') for Nylon 6 Fiber

Draw ratio	n_{iso}	$\sigma \times 10^{-3}$	$\varepsilon^{\parallel}$	$\varepsilon^{\perp}$	$\bar{\varepsilon}$	$\eta^{\parallel} \times 10^{-2}$	$\eta^{\perp} \times 10^{-2}$	$\bar{\eta} \times 10^{-2}$	R'
1.00	1.5432	11.288	2.397	2.374	2.381	11.119	10.930	10.992	2.350
1.23	1.5411	11.260	2.402	2.362	2.375	11.156	10.836	10.942	2.335
1.46	1.5428	11.304	2.428	2.357	2.380	11.366	10.795	10.983	2.347
1.69	1.5405	11.264	2.422	2.349	2.373	11.314	10.736	10.927	2.331
1.92	1.5414	11.286	2.434	2.347	2.376	11.411	10.722	10.949	2.337
2.15	1.5410	11.293	2.451	2.338	2.375	11.545	10.644	10.939	2.334
2.38	1.5409	11.297	2.459	2.333	2.374	11.610	10.610	10.937	2.334

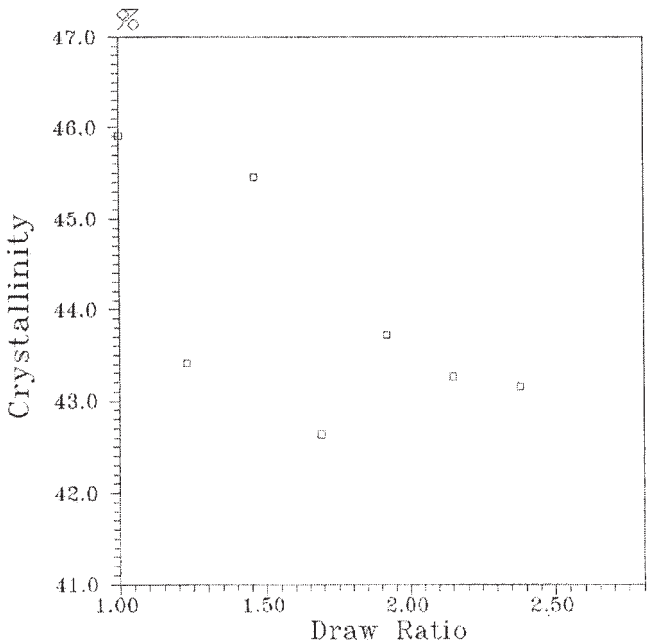

Figure 4 Relationship between crystallinity X_v with draw ratio for nylon 6 fiber.

as the result of new orientation and the average optical orientation functions F_{av}. The average orientation function increases with increasing draw ratio for nylon 6 fibers.

Figures 8 and 9 show the increase in the stress optical coefficient C_s for nylon 6 fibers resulting from

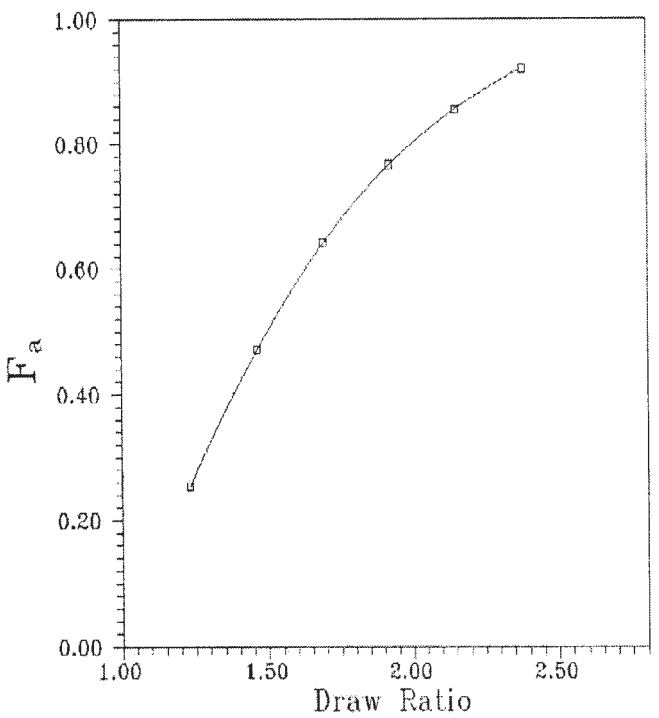

Figure 5 Relationship between the amorphous orientation function F_a and draw ratio for nylon 6 fibers.

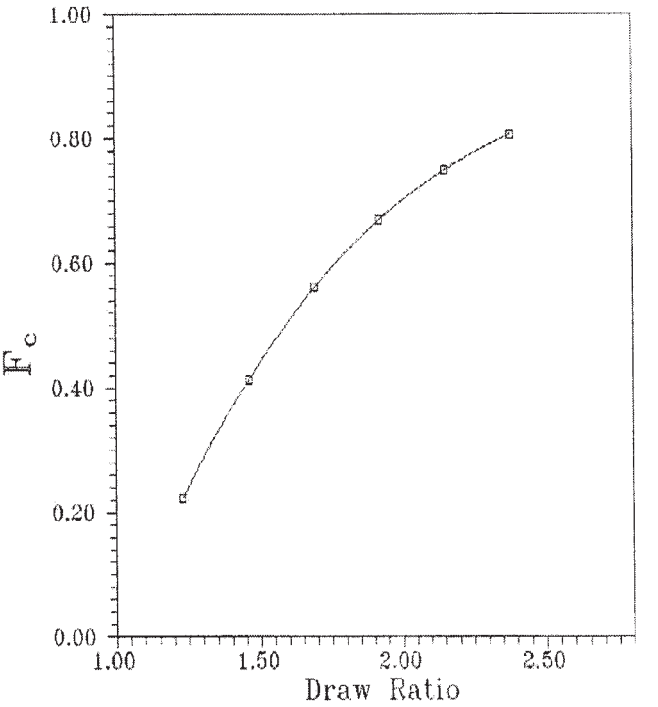

Figure 6 Relationship between the crystalline orientation function F_c and draw ratio for nylon 6 fibers.

increasing draw ratio and the molar number of chain segments per unit volume (N_e) for nylon 6 fibers. N_e decreased as the draw ratio increased and the shrinkage stress k_s for nylon 6 fibers increased as the draw ratios increased (Fig. 10).[11]

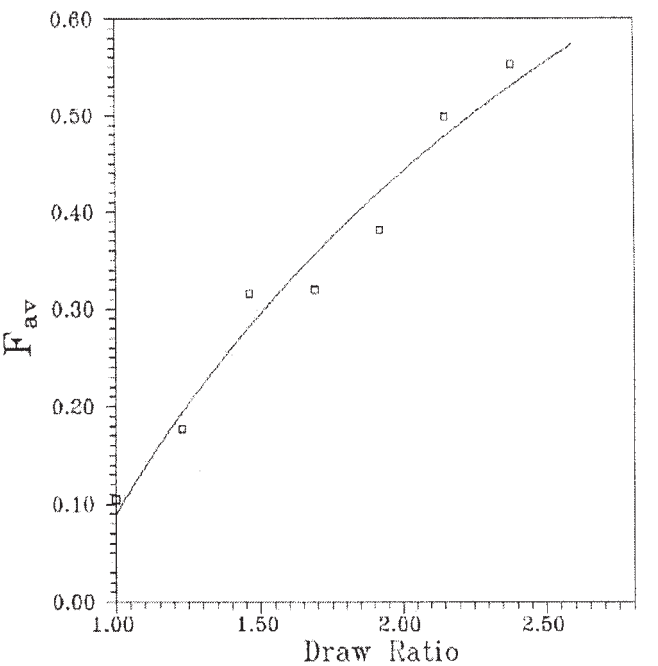

Figure 7 Relationship between average orientation F_{av} and draw ratio for nylon 6 fiber.

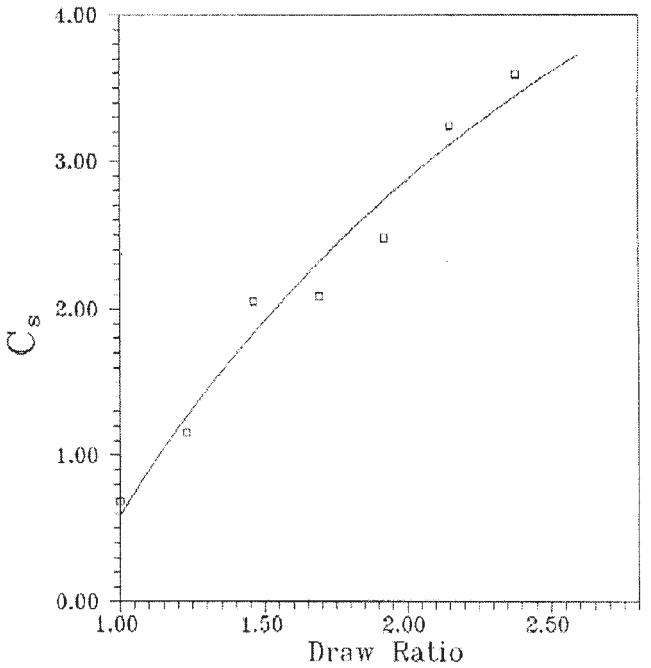

Figure 8 Stress optical coefficient C_s plotted against draw ratio for nylon 6 fiber.

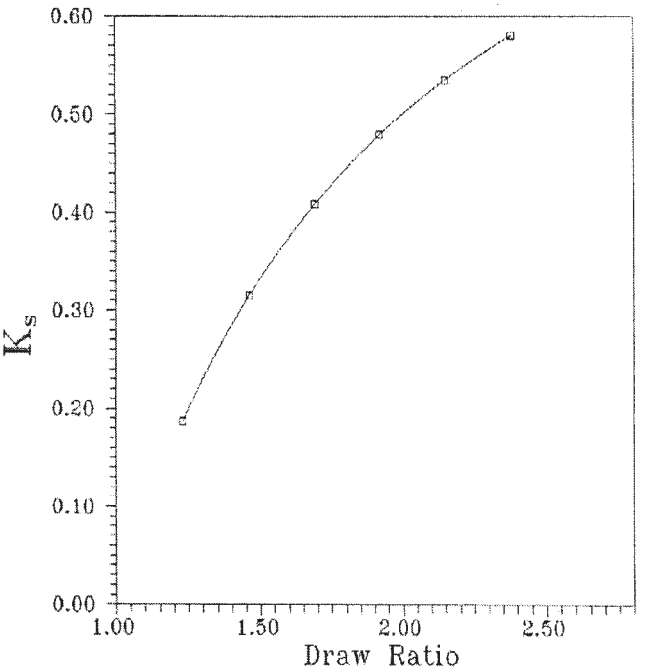

Figure 10 Relationship between draw ratio and the shrinkage stress k_s for nylon 6 fiber.

The surface reflectivity (R') and the tensile stress (σ) were calculated and the resultant data are given in Table I.

An isotropic polymer has the same structure and properties in all directions upon deformation in the solid state, and the polymer becomes anisotropic because the polymer chains align and therefore become oriented with respect to a particular direction. The degree of orientation, crystallinity, and other structural parameters are correlated to the final fiber end use. Thus, optical birefringence gives the average of crystalline and amorphous orientation. Orientation frequently means orientations of ordered phases. Much effort has gone toward clarifying the molecular orientation characteristics of semicrystalline polymers, which usually form not only a crystalline phase but also an amorphous phase in the solid state. Whereas the degree of orientation always increases in the course of drawing, the crystallinity can change in both directions. Three types of behavior can be distinguished[36]:

1. Deformation is accompanied by additional crystallization and an increase of crystallization.
2. Deformation does not affect phase structure: an undrawn amorphous sample remains amorphous after drawing; a crystalline sample does not change its degree of crystallinity.
3. Deformation is accompanied by partial destruction of the original structure and reduction of crystallinity.

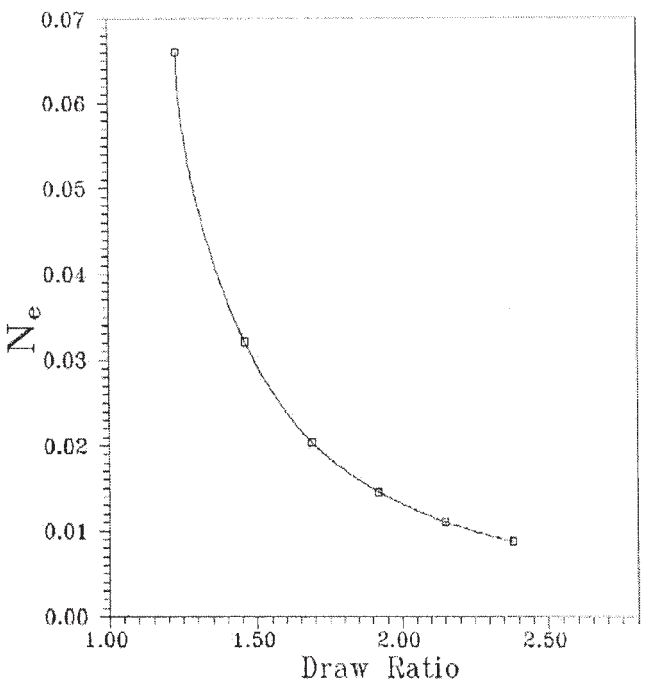

Figure 9 Relationship between draw ratio and the molar number chain segments per unit volume N_e for nylon 6 fiber.

Thus, the present crystallinity results show a reduction in the degree of original fiber crystallinity (Fig. 4) attributed to cold drawing, which may in turn arise from the drastic distortion of the original structure of the amorphous, material phase.

The morphology of polyamide-6 has been investigated by various groups and a considerable number of articles have been published in the literature in recent years on the subject of microstructural characterization of polyperamide-6 fibers and films by various characterization techniques.[31] It is evident that changes in the density of polyamide-6 with an increasing draw ratio can be interpreted as changes in the crystal from the total crystallinity, or both.[36]

As shown from eqs. (4a) and (4b), the crystalline and amorphous orientation functions (F_c and F_a) were calculated. In Figures 5 and 6, the crystalline and amorphous orientation functions are plotted against the draw ratios. Concerning the crystalline orientation (F_c), the increase of the draw ratio from 1.0 to 2.380 elicited only an approximately 75% increase in the value of F_c; however, it has a high value, even at the lower draw ratio. On the other hand, in the corresponding range of elongation, the amorphous orientation function F_a increased more significantly with increasing draw ratio. Also both F_c and F_a, shown Figures 4 & 5, respectively, substantially depend on the draw ratio, in the case of stretching of nylon 6 fibers. Under a given external force, the mechanical anisotropy for crystalline polymers and glassy polymers, deformed by cold drawing, enables the factors $[P_4(\cos\theta)]$ and $[P_2(\cos\theta)]$ to be calculated as a function of draw ratio. On the aggregate model the low strain mechanical anisotropy is related to the orientation functions $[P_2(\cos\theta)]$ and $[P_4(\cos\theta)]$. These functions provide some understanding of the mechanism of deformation. It is notable that $[P_2(\cos\theta)]$ and $[P_4(\cos\theta)]$ [Fig. 3(a) and (b)] values are decreased with the increasing draw ratios related to the state degree of crystallinity (Fig. 4). Even as deformation of the present samples of nylon 6 fibers consists of destruction of the original structure and rebuilding of a new structure, so the mechanical anisotropy for polymeric materials depends on the deformation and accompanying state of crystallinity.[7] The difference in their values, by comparison with this for F_{av}, perhaps arises because the factors $[P_2(\cos\theta)]$ and $[P_4(\cos\theta)]$ are functions only of the draw ratios.

From another perspective of interpretation, the change in the obtained results of ε, η, $\bar{n}$, and R' may be attributable to modification in the electrical properties arising from the existing space charges and remnant electric field in polymers after preparation. Furthermore, application of the Mooney–Rivlin coefficients can allow estimation for both N_0, the crosslink density, and N_s, the chain entanglement density. Calculation of values of the N_e parameter (i.e., the molar number of chain segments per unit volume) helps to explain the losses attributed to stress–strain variations.

By the shrinkage stress (k_s) information, it has been possible to determine the controlling mechanism in shrinkage of nylon 6.

CONCLUSIONS

It is clear that the two-beam technique is useful for clarifying the optical behavior mechanism of nylon 6 fibers with different draw ratios. From the obtained results the following conclusions are reported.

1. The factor $\langle P_4(\cos\theta)\rangle$ is always comparatively small. So the mechanical method could be used to determine the orientation parameters $\langle P_2(\cos\theta)\rangle$ and $\langle P_4(\cos\theta)\rangle$. The optical and mechanical orientation techniques are suitable for conferring variations on molecular orientation parameters.
2. Changes in orientation are accompanied by a change of crystallinity resulting from the cold-drawing process, which indicates mass redistribution within the fiber chain.
3. Both the shrinkage stress (k_s) and the stress optical coefficient (C_s) increase as the draw ratio increases, whereas the molar number of chain segments per unit volume (N_e) decreases as the draw ratio increases; thus the crosslink density relies substantially on the draw ratio because crystallites act as a physical cross point. Moreover, the crosslink density (N_0) and the chain entanglement density (N_s) were calculated as the draw ratio increased.
4. The obtained principal optical parameters are suitable for evaluating the dielectric constant, the dielectric susceptibility, and surface reflectivity in nylon 6 fibers.
5. Both crystalline (F_c) and amorphous orientation function (F_a) increased as the draw ratio increased.

From the preceding results and considerations, we concluded that the drawings are sensitive to varying optical structural parameters and other physical properties in polymeric materials, such that they acquire new reorientation factors and structural parameters.

References

1. Whitney, W.; Andrews, R. D. J Polym Sci 1967, B5, 251.
2. Whitney, W.; Andrews, R. D. J Polym Sci 1967, C16, 2981.
3. Duckett, R. A.; Rabinowitz, S.; Ward, I. M. J Mater Sci 1970, 5, 909.
4. Billmeyer, F. W., Jr., Text Book of Polymer Science, 3rd ed.; Wiley–Interscience: New York, 1965; p. 168.
5. Hermans, P. H. Contributions to the Physics of Cellulose Fibers; North-Holland: Amsterdam, 1946; Chapters 3 and 4.
6. Samules, R. J. Structural Polymer Properties; Wiley: New York, 1974; pp. 20, 51, 63, 219.
7. Ward, I. M. J Polym Sci Polym Symp 1977, 58, 5.
8. Suzuki, A.; Murata, H.; Koito, K. J Polym Sci Part B: Polym Phys 2000, 38, 1137.
9. Suzuki, A.; Murata, H.; Kunugi, T. Polymer 1998, 39, 1351.
10. Zachariodes, A. E.; Porter, S. J Appl Polym Sci 1979, 24, 1371.
11. Coate, P. D.; Ward, I. M. J Mater Sci 1978, 13, 1957.
12. Coate, P. D.; Ward, I. M. J Mater Sci 1980, 15, 2897.

13. Suzuki, A.; Kawada, T.; Hasegawa, T. J Polym Sci Part B: Polym Phys 2001, 39, 1629.
14. Williams, D. J. Polymer Science and Engineering; Prentice-Hall: Englewood Cliffs, NJ, 1971; p. 191.
15. Bodor, G. Structural Investigation of Polymers; Ellis Horwood: New York, 1991; p. 215.
16. John, V. B. Introduction to Engineering Materials; Macmillan: London, 1972; p. 74.
17. Pluta, M. J Microsc 1972, 96, 309.
18. Barakat, N.; Hamaza, A. A. Interferometry of Fibrous Materials; Hilger: Bristol, UK, 1990.
19. Pluta, M. Optica Acta 1971, 18, 661.
20. Fouda, I. M. J Polym Res 2002, 1.
21. Hamaza, A. A.; El-Farahaty, K. A.; Hellaly, S. A. Optica Appl 1988, 18, 133.
22. Wunderlich, B. Macromolecular Physics, Vol. 1, Crystal Structure, Morphology, and Defects; Academic Press: London, 1973; p. 426.
23. Gaur, G. H. A.; de Vries, H. J Polym Sci Polym Phys Ed 1975, 15, 835.
24. Holmes, D. R.; Bunn, C. W.; Smith, D. J. J Polym Sci 1955, 17, 159.
25. Roldan, L. G.; Kaufman, G. S. J Polym Sci Part B: Polym Phys 1963, 3, 1603.
26. Le Bourvelles, G.; Beautemps, J. J Appl Polym Sci 1990, 39, 329.
27. Kungi, T.; Yokokura, S.; Hashimoto, M. Nippon Kagaku Kaishi 1976, 2, 278 [cited in Suzuki, A.; Murata, H.; Koito, K. J Polym Sci Part B: Polym Phys 2000, 38, 1137].
28. Wesolowska, E.; Lewaskiewicz, W. J Polym Sci Polym Phys Ed 1988, 26, 2573 [cited in Murthy, N. S.; Bray, R. G.; Carreale, S. T.; Moore, R. A. F. Polymer 1995, 36, 3863].
29. Riande, E.; Guzman, J. J Polym Sci Polym Phys Ed 1984, 22, 917.
30. Gedde, U. F. W. Polymer Physics; Chapman & Hall: London, 1997; p. 47.
31. Moony, M. J Appl Phys 1940, 11, 582; Moony, M. J Appl Phys 1948, 19, 434; Rivlin, R. S. Trans R Soc London A Phys Sci 1948, A241, 379 [all cited in Gedde, U. F. W. Polymer Physics; Chapman & Hall: London, 1997].
32. Ball, R. C.; Doi, M.; Edward, S. F.; Warner, M. Polymer 1981, 22, 1010 [cited in Mattews, R. G.; Duckett, R. A.; Ward, I. M.; Jones, D. P. Polymer 1997, 38, 4795].
33. Helmsley, D. A. Applied Polymer Light Microscopy; Elsevier: London, 1987; pp. 7, 193.
34. Fouda, I. M.; Shabana, H. Polym Test 2001, 20, 441.
35. Walezak, Z. K. Formation of Synthetic Fibers; Gordon & Breach: New York, 1977; p. 418.
36. Vasanthan, N.; Salem, D. R. J Poly Sci Part B: Polym Phys 2001, 39, 536.